International Symposium on New Developments in Advanced High Strength Sheet Steels (AHSS 2013)
Colorado,US, Jul 2013

Microstructure Engineering of Dual-Phase Steels

M. Militzer, W.J. Poole, T. Garcin, M. Kulakov and B. Zhu

The University of British Columbia, The Centre for Metallurgical Process Engineering,
309-6350 Stores Road, Vancouver, B.C. Canada V6T 1Z4
Email: Matthias.militzer@ubc.ca

Key Words: Intercritical annealing, process modeling, phase field model, recrystallization, austenite formation, austenite decomposition

INTRODUCTION

Dual-phase (DP) steels have become a material of choice for automotive manufacturers due to their attractive combination of strength and forming characteristics.[1] The required microstructure for these steels is usually obtained through intercritical annealing of the cold-rolled steel in a hot-dip galvanizing line (HDGL). Mechanical properties of dual-phase steels are characterized by continuous yielding, large work-hardening rate and good formability. Yield and tensile strengths increase with the martensite content.[2] A martensite content of approximately 15-20% is typically desired to have sufficiently large uniform elongation of automotive sheets. Refinement of martensite island size has been shown to increase both work-hardening rate and uniform elongation.[3,4] Further, a uniform distribution of equiaxed martensite particles leads to improvements in uniform elongation and damage accumulation.[5,6] Therefore, a microstructure process model for intercritical annealing must be capable to predict in addition to the fraction of microconstituents in the final microstructure their size and distribution. Individual models have been developed for recrystallization, austenite formation and decomposition taking place during the intercritical annealing cycle.[7-9] Using a 3D cellular automaton (CA) approach Bos et al.[10] have linked the individual models for these three microstructure phenomena to describe the entire microstructure evolution process. In their approach, however, austenite formation is described as an interface controlled reaction and long-range carbon diffusion is not taken into account.

The goal of the present study is the development of an improved microstructure evolution model for the intercritical annealing cycle. The present paper describes the status of the model development and its application to intercritical annealing for a selected low-carbon steel that is suitable for industrial production of a DP 600 grade. First, experimental studies are described to quantify the effects of annealing parameters on recrystallization and phase transformations. Then, the concept of microstructure engineering is used to model the microstructure evolution as a function of the industrial processing path. In this approach a set of semi-empirical models for recrystallization, austenite formation and decomposition are formulated based on the Johnson-Mehl-Avrami-Kolmogorov (JMAK) equation. In addition, a meso-scale phase field model (PFM) is proposed to mitigate some of the limitations of the JMAK approach.

EXPERIMENTAL STUDIES

The goal of the experimental studies was to determine the material specific parameters for recrystallization, austenite formation and austenite decomposition. Subsequently, annealing simulations were conducted to evaluate and validate the proposed models. In the present study, a low-carbon steel was investigated with a typical DP600 grade chemistry, as shown in Table I. The industrially processed steel was received from ArcelorMittal Dofasco Inc. in form of 1.8 mm thick 50 pct cold-rolled sheets with a ferrite-bainite-pearlite microstructure, as shown in Figure 1. Heat treatments of samples cut from these sheets were conducted using a Gleeble 3500 thermomechanical simulator. The heat treatments included isothermal, continuous heating and cooling tests as well as simulations of the entire annealing cycle. The recrystallization kinetics was quantified metallographically. Austenite formation and decomposition kinetics were measured in-situ with a dilatometer. The microstructures of both recrystallization and phase transformation samples were analyzed using standard metallographic procedures and employing optical and scanning electron microscopy. A more detailed description of the experimental

procedures can be found elsewhere.[11] In addition to these standard techniques, laser ultrasonics for metallurgy (LUMet) was employed as a new technique to in-situ monitor microstructure evolution. For this purpose, a LUMet system was attached to the rear door of the Gleeble. The details of the experimental setup of the LUMet system are described elsewhere.[12]

Table I. Major alloying elements in the investigated steel (wt. pct)

C	Mn	Si	Cr
0.105	1.858	0.157	0.340

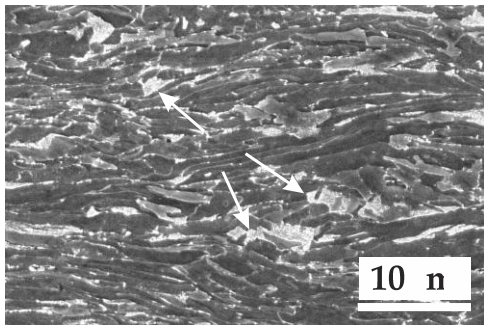

Figure 1. Microstructure of cold-rolled sheets (P indicates pearlite)

The results of the recrystallization and austenite formation studies can be found in our previous publications that also include the JMAK models for recrystallization and austenite formation.[11,12] There are two important findings from these experimental studies: (i) Laser ultrasonics is a suitable technique to monitor recrystallization in-situ. (ii) There is a critical heating rate above which recrystallization is not completed before the onset of austenite formation. Figure 2 gives examples of comparing metallographic recrystallization measurements with the evolution of ultrasonic velocity as obtained with LUMet during isothermal and continuous heating experiments. Clearly, an ultrasonic velocity change is observed when recrystallization is taking place. This can be attributed to texture changes during recrystallization.[13,14] In the present case, completion of recrystallization can be reliably captured with LUMet but not the start of recrystallization, i.e. recrystallization is recorded with laser ultrasonics once the recrystallized fraction is above approximately 0.30. Figure 3 shows the effect of heating rate on recrystallization. Increasing the heating rate shifts recrystallization to higher temperatures. When the heating rate to the intercritical region exceeds 7 °C/s recrystallization of the cold-rolled structure is not yet completed before the onset of austenite formation that regardless of heating rate starts at approximately 730 °C. Whether or not recrystallization and austenite formation occur sequentially or simultaneously has significant effects on the formation rate and morphology of intercritical austenite. Figure 4 shows examples of intercritical microstructures when austenite forms from recrystallized and non-recrystallized ferrite, respectively. The distribution of austenite can be inferred from the martensite in the microstructure that was obtained upon quenching the samples. A necklace type austenite morphology is evident when austenite forms from recrystallized ferrite (see Figure 4a), whereas randomly distributed equiaxed austenite grains result when austenite forms from non-recrystallized ferrite (see Figure 4b). To obtain 50% austenite at 770 °C the annealing time was 600 s in the recrystallized and 90 s in the non-recrystallized material, respectively. The increased austenite formation rate from the unrecrystallized structure can be attributed to an increase in the nuclei density and the presence of fast diffusion paths.[11]

The austenite decomposition was studied from intercritical austenite (with 50% austenite) using typical cooling conditions for a HDGL, i.e. cooling at 3, 10 and 30 °C/s to the zinc bath temperature of 465 °C where samples were held for 180 s. It was found that the decomposition kinetics depends on the degree of recrystallization completion prior to austenite formation. Figure 5 provides an example for the austenite decomposition kinetics during cooling and holding. Initially, epitaxial ferrite forms from the pre-existing ferrite in the microstructure and for sufficiently low transformation temperatures bainite forms instead of ferrite. The austenite remaining after holding at 465 °C will primarily transform to martensite upon further cooling to room temperature.

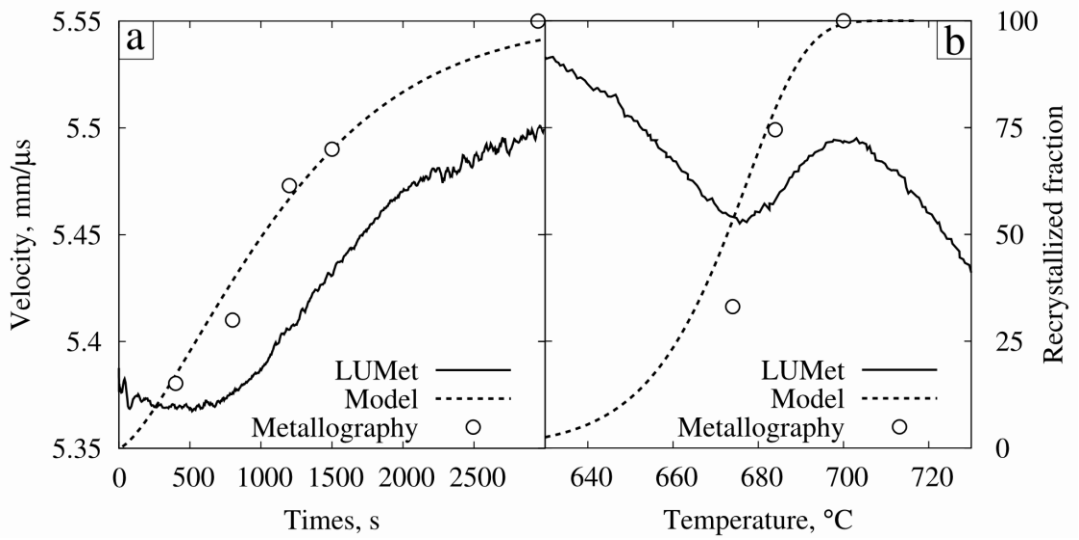

Figure 2: Comparison of laser ultrasonic velocity with fraction recrystallized during (a) isothermal holding at 600 °C and (b) continuous heating at 1 °C/s

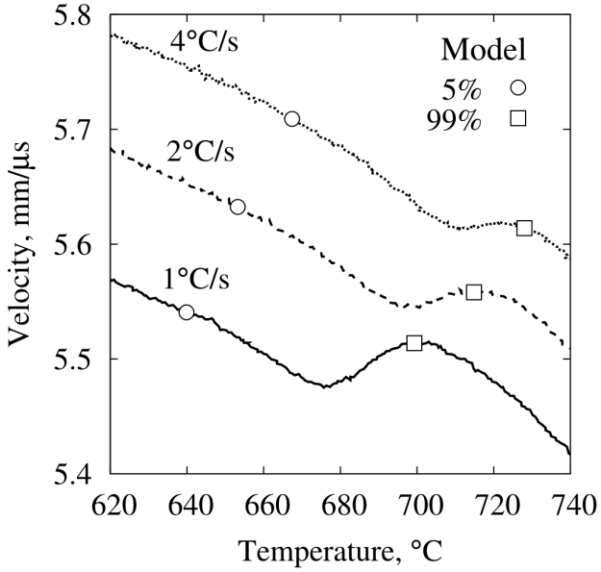

Figure 3. Effect of heating rate on recrystallization kinetics (as measured with ultrasonic velocity and predicted by the model) during continuous heating. For the sake of clarity, offsets of 0.1mm/µs are applied on the velocity curves for 2 and 4 °C/s.

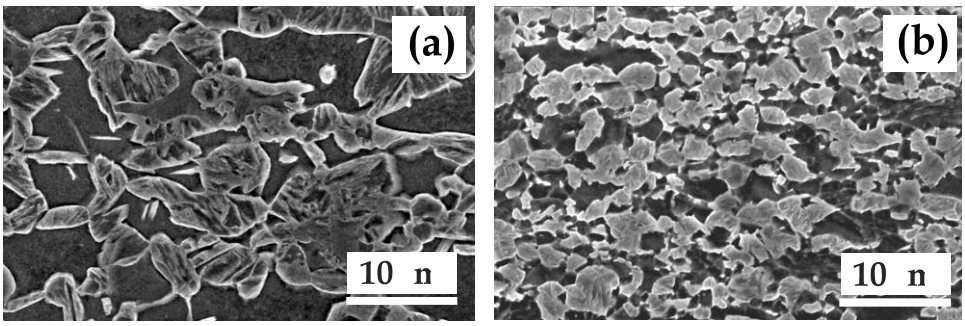

Figure 4. Intercritical austenite microstructures (50 pct ferrite – 50 pct austenite) formed at 770 ºC from (a) recrystallized ferrite, (b) non-recrystallized ferrite (F: ferrite, M: martensite)

PHENOMENOLOGICAL ANNEALING MODEL

The Johnson-Mehl-Avrami-Kolmogorov (JMAK) model was employed to describe the recrystallization and phase transformation kinetics, i.e. for the isothermal case:

$$X = 1 - \exp(-b \cdot t^n) \quad [1]$$

where X is the volume fraction recrystallized/transformed, b is a rate parameter, t is time and n is the JMAK exponent. As described elsewhere,[11] the temperature dependence of the parameter b for recrystallization and austenite formation is given by an Arrhenius expression:

$$b = b_0 \exp(-Q / RT) \quad [2]$$

with the pre-exponential factor, b_0, the effective activation energy, Q, the ideal gas constant, R, and the absolute temperature, T. The three adjustable model parameters n, b_0 and Q were determined based on the experimental results as presented elsewhere.[11] In case of recrystallization, the adjustable parameters were determined from the isothermal studies and then the additivity principle was applied to predict the recrystallization kinetics during continuous heating. As illustrated in Figures 2b and 3, the predictions of the model are in good agreement with the experimentally measured recrystallization kinetics for continuous heating confirming the additive nature of the recrystallization process. Similarly, austenite formation from recrystallized ferrite can be described using the JMAK theory and the additivity principle. When, austenite forms from non-recrystallized or partially recrystallized ferrite the reaction cannot be described assuming additivity, as now both austenite formation and ferrite recrystallization occur concurrently. Thus, the proposed phenomenological annealing model is only applicable as long as the heating rate is below the critical rate of 7 °C/s.

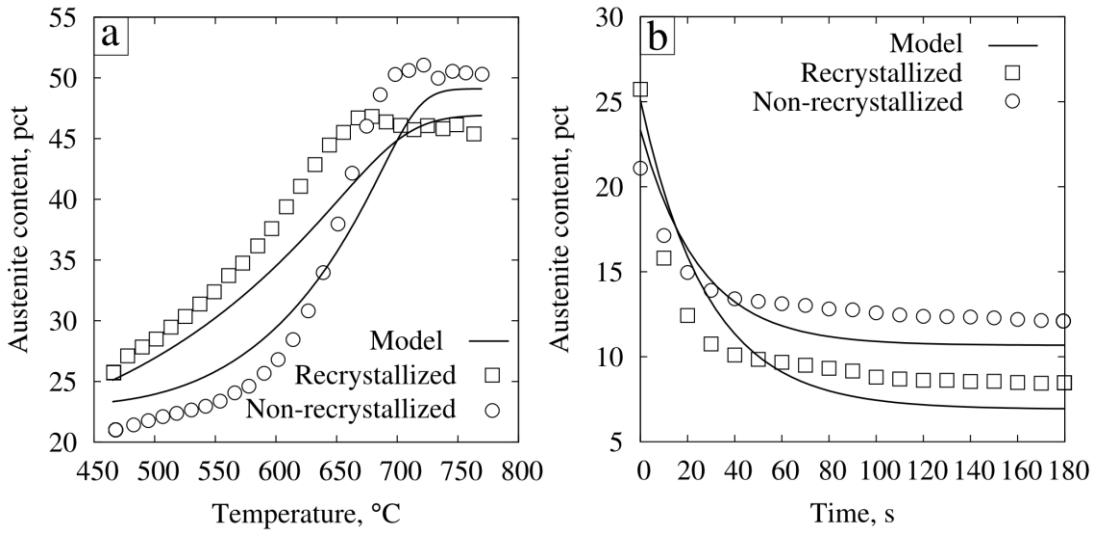

Figure 5. Kinetics of austenite decomposition during (a) cooling at 30 ºC/s and (b) holding at 465 ºC

The JMAK approach and additivity is also applied to describe the formation of epitaxial ferrite and bainite during continuous cooling. Further, the JMAK theory can be used to describe the bainite formation during isothermal holding at 465 ºC. The model parameters for austenite decomposition are summarized in Table II and the fit quality is illustrated in Figure 5. The calculated austenite content is within 5 pct of that measured by dilatometry. The transformation parameters depend on whether ferrite is recrystallized or not recrystallized before the onset of austenite formation. During continuous cooling, the model for the formation of epitaxial ferrite remains applicable to the bainite portion. In accordance with experimental observations the start of bainite formation is implemented when the fraction of remaining austenite, f_γ, reaches 0.30. For the

isothermal bainite reaction the JMAK equation is renormalized by introducing a maximum fraction of bainite, B_{max}, that is a function of the fraction of remaining austenite, $f_\gamma(0)$, when reaching 465 ºC.

The overall microstructure model has been validated by comparing measured and predicted microstructures for selected laboratory simulated annealing cycles that are typical for DP steel processing in an industrial HDGL. An example of this validation is shown in Figure 6. During the annealing simulation recrystallization was measured in-situ with the LUMet system whereas austenite formation and decomposition were recorded by dilatometry. The resulting final microstructure is shown in Figure 7 and consists of a complex multi-phase structure that includes ferrite, bainite and martensite. Table III provides the details of measured and predicted microstructure constituents confirming very good agreement of the model with the annealing simulation.

Table II. Parameters for austenite decomposition model*

Recrystallized material	Non-recrystallized material
Austenite decomposition during cooling (epitaxial ferrite and bainite)	
$n = 0.1$	$n = 0.05$
$b = 0.82 + 0.003 \cdot T - 0.44 \cdot 10^{-5} \cdot T^2$	$b = -1.9 + 0.0133 \cdot T - 1.33 \cdot 10^{-5} \cdot T^2$
Bainite starts to form when $f_\gamma = 0.30$	
Bainite formation during holding at 465 ºC holding	
$n = 1$ $b = 0.003 \cdot f_\gamma(0) - 0.04$ $B_{max} = 2 \cdot f_\gamma(0) - 0.32$	$n = 1$ $b = 0.006 \cdot f_\gamma(0) - 0.1$ $B_{max} = 2 \cdot f_\gamma(0) - 0.34$

*b is in s^{-n}, T is in ºC.

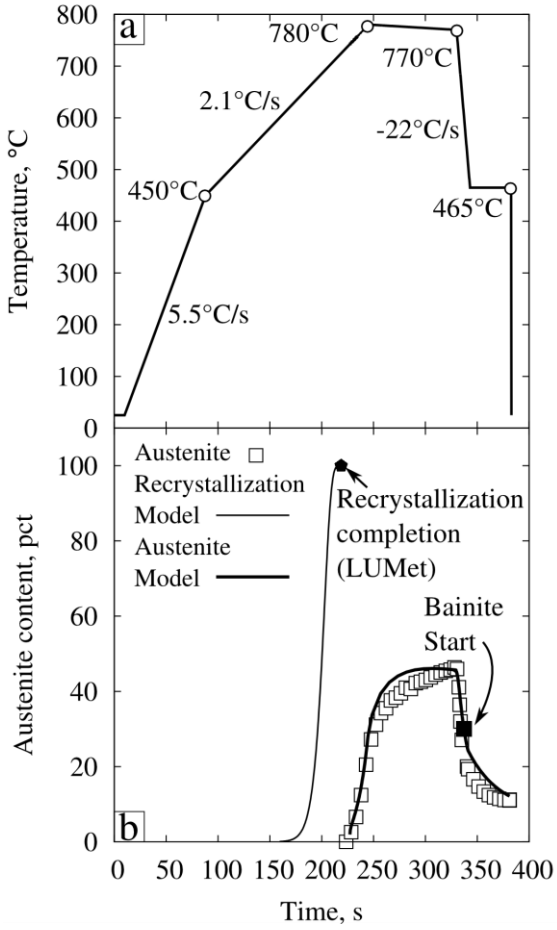

Figure 6. (a) Thermal path for industrial processing of DP600 steel, (b) corresponding microstructure evolution

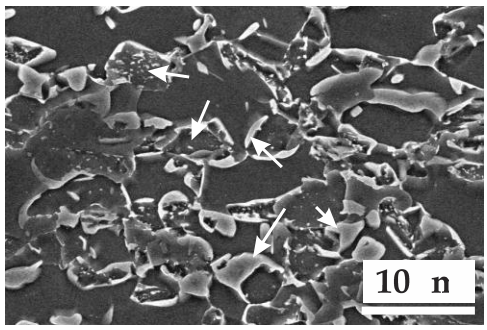

Figure 7. Final microstructure after simulation of the industrial intercritical annealing process (F: ferrite, B: bainite, M: martensite)

Table III. Microconstituent contents in the final microstructure for the simulated annealing cycle

Microconstituent	Experiment, pct	Model, pct
Intercritical ferrite	54	54
Epitaxial ferrite	18	16
Bainite	17	18
Martensite	11	12

PHASE FIELD MODEL

As size, distribution and morphology of microstructure constituents may significantly affect DP steel properties, a multi-phase field model[15] was also employed to describe the microstructure evolution during intercritical annealing. An advantage of this meso-scale model, as compared e.g. to the Cellular Automaton approach, is the ability to naturally handle complex morphologies of various constituents.[16] Further, an important advantage of meso-scale models compared to the JMAK approach is the ability to visualize microstructures. For simplicity, the cold-rolled structure was approximated with a ferrite-pearlite starting microstructure in the phase field model (PFM) simulations. Pearlite was considered as a pseudo homogeneous phase with the eutectoid carbon concentration of 0.63 wt. pct. The phase field modeling of ferrite recrystallization was presented in detail in a previous paper.[14] Figure 8 shows 2D PFM domains of the initial cold rolled structure and the simulation result after completion of ferrite recrystallization during heating at 1 ºC/s. Both conditions, i.e. non-recrystallized and recrystallized, were taken as initial structures for 2D PFM simulations of austenite formation.

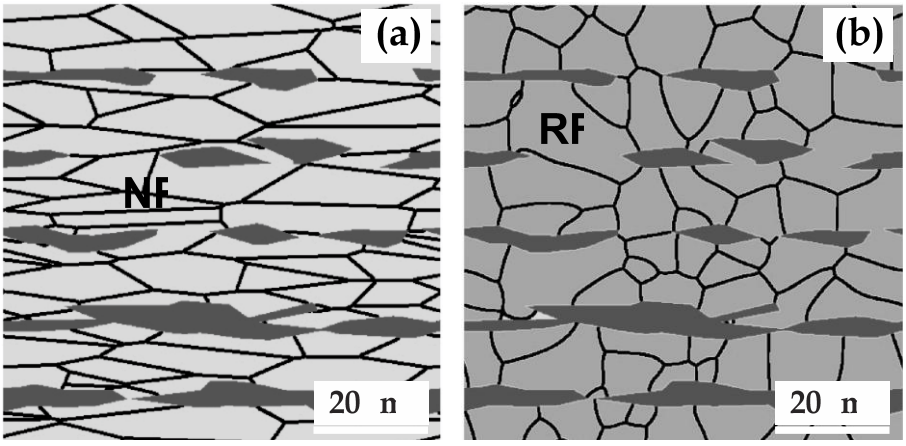

Figure 8. (a) Initial PFM microstructure representing the cold-rolled state, (b) PFM simulated recrystallized microstructure after heating at 1 ºC/s to 720 ºC (NR: non-recrystallized ferrite, RF: recrystallized ferrite, P: pearlite)

In the PFM for austenite formation, para-equilibrium conditions were assumed, i.e. only partitioning of carbon by long-range diffusion was considered, and the multi-phase field equations were coupled with the diffusion equation for carbon.[16] All thermodynamic data were obtained from ThermoCalc using the FE-2000 database.[17] Based on metallographic observations austenite nuclei were introduced in two stages. At a temperature of 730 ºC austenite nucleated at the boundaries of pearlite colonies; completion of pearlite dissolution was followed by austenite nucleation at ferrite grain boundaries at 770 ºC. In case of partial ferrite recrystallization, it was assumed that no austenite nuclei form at the moving ferrite grain boundaries of a recrystallizing grain. The model was fit to austenite formation kinetics by adjusting the nucleation scenarios and the mobilities of the austenite-ferrite and austenite-pearlite interfaces. The overall austenite formation kinetics could reasonably be described with the PFM when (i) a Mn solute drag term was introduced for the effective mobility of the austenite-ferrite interface as suggested by Fazeli and Militzer[18] and (ii) the mobility of the austenite-pearlite interface was increased with the fraction of non-recrystallized ferrite at the onset of austenite formation. The consideration of solute drag enabled to describe the ferrite-to-austenite transformation with an interface mobility that depends both on temperature and interface velocity. The mobility of the pearlite-austenite interface was assumed to have an Arrhenius-type temperature dependence with an activation energy of 360 kJ/mol. The pre-exponential mobility term was increased by a factor 5 for non-recrystallized ferrite (Figure 10) as compared to completely recrystallized ferrite (Figure 9) to account for the acceleration of austenite formation from the non-recrystallized structure. Further, the PFM simulations reasonably replicated morphology and distribution of intercritical austenite as seen from partially austenitized microstructures, Figures 9 and 10. A minor discrepancy is the shape of austenite formed at ferrite grain boundaries. In the simulations the shape is more equiaxed (Figure 9b) while the micrograph shows austenite allotriomorphs growing preferentially along ferrite grain boundaries. A possible reason for this difference may be that fast diffusion paths along grain boundaries were not considered in the simulations.

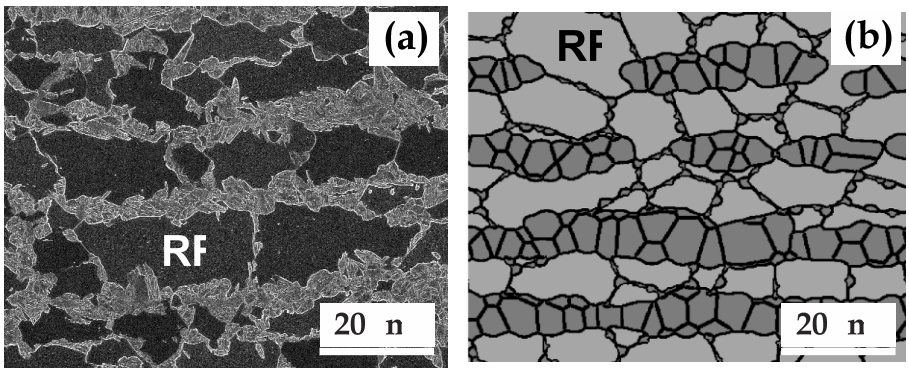

Figure 9. Austenite morphology after continuous heating at 1 ºC/s to 790 ºC (a) experimental micrograph and (b) microstructure obtained by PFM simulation (RF: recrystallized ferrite, M: martensite, A: austenite)

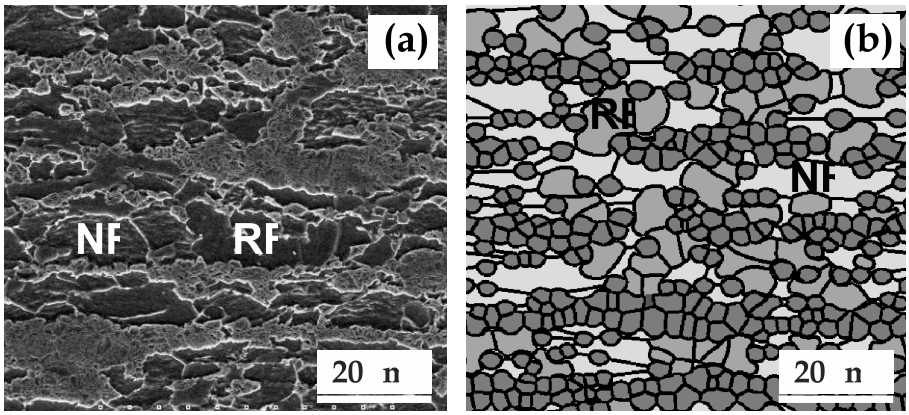

Figure 10. Austenite morphology after continuous heating at 100 ºC/s to 795 ºC (a) experimental micrograph and (b) microstructure obtained by PFM simulation (RF: recrystallized ferrite, NR: non-recrystallized ferrite, M: martensite, A: austenite)

SUMMARY

Extending the concept of microstructure engineering, i.e. modeling the microstructure evolution as a function of the industrial processing path, a microstructure process model has been developed for intercritical annealing of a DP 600 steel on a hot-dip galvanizing line. The model was validated with in-situ microstructure observations using laser ultrasonics and dilatometry in laboratory simulated annealing cycles. A limitation of the proposed process model is that, in its current form, it cannot account for rapid annealing cycles where recrystallization and austenite formation overlap. Thus, a phase field model approach was adopted that describes the interaction of recrystallization and austenite formation and, moreover, predicts microstructures with spatial resolution.

ACKNOWLEDGEMENT

The authors acknowledge the financial support received from the Natural Sciences and Engineering Research Council of Canada (NSERC) and ArcelorMittal Dofasco Inc. (Hamilton, ON, Canada).

REFERENCES

1. Steel Market Development Institute: ULSAB-AVC (Advanced Vehicle Concepts), 2002.
2. R. Davies, "Influence of Martensite Composition and Content on the Properties of Dual Phase Steels," *Metallurgical and Materials Transactions A,* Vol. A9, 1978, pp. 671-679.
3. N.K. Balliger and T. Gladman, "Work Hardening of Dual-Phase Steels," *Metal Science,* Vol. 15, 1981, pp. 95-108.
4. C.A.N. Lanzillotto and F.B. Pickering, "Structure-Property Relationships in Dual-Phase Steels," *Metal Sceince,* Vol. 16, 1982, pp. 371-382.
5. G. Avramovic-Cingara, Y. Ososkov, M.K. Jain and D.S. Wilkinson, "Effect of Martensite Distribution on Damage Behaviour in DP600 Dual Phase Steels," *Materials Science and Engineering A,* Vol. A516, 2009, pp. 7-16.
6. M. Mazinani and W.J. Poole, "Effect of Martensite Plasticity on the Deformation Behavior of a Low-Carbon Dual-Phase Steel," *Metallurgical and Materials Transactions A,* Vol. A38, 2007, pp. 328-339.
7. M. Militzer, "Computer Simulation of Microstructure Evolution in Low Carbon Sheet Steels," *ISIJ International,* Vol. 47, 2007, pp. 1-15.
8. D. Raabe and L. Hantcherli, "2D Cellular Automaton Simulation of the Recrystallization Texture of an IF Sheet Steel under Consideration of Zener Pinning," *Computational Materials Science,* Vol. 34, 2005, pp. 299-313.
9. J. Rudnizki, B. Böttger, U. Prahl and W. Bleck, "Phase-Field Modeling of Austenite Formation from a Ferrite plus Pearlite Microstructure during Annealing of Cold-Rolled Dual-Phase Steel," *Metallurgical and Materials Transactions A,* Vol. A42, 2011, pp. 2516-2525.
10. C. Bos, M. Mecozzi, D. Hanlon, M. Aarnts and J. Sietsma, "A Microstructure Model for Recrystallisation and Phase Transformation during the Dual-Phase Steel Annealing Cycle," *Metallurgical and Materials Transactions A,* Vol. A42, 2011, pp. 3602-3610.
11. M. Kulakov, W.J. Poole and M. Militzer, "The Effect of the Initial Microstructure on Recrystallization and Austenite Formation in a DP600 Steel," *Metallurgical and Materials Transactions A,* 2013, in press.
12. M. Militzer, T. Garcin and W.J. Poole, "In-situ Measurements of Grain Growth and Recrystallization by Laser Ultrasonics" *5th International Conference on Recrystallization & Grain Growth*, Sydney, Australia, 2013, in press.
13. S.E. Kruger, G. Lamouche, A. Moreau and M. Militzer, "Laser Ultrasonic Monitoring of Recrystallization of Steels", *Materials Science and Technology 2004 Conference Proceedings*, TMS, Warrendale, PA, pp. 809-813.
14. B. Zhu and M. Militzer, "3D Phase Field Modelling of Recrystallization in Low-carbon Steel", *Modelling and Simulation in Materials Science and Engineering*, Vol. 20, 2012, 085011 (17pp).
15. J. Eiken, B. Böttger and I. Steinbach, "Multiphase-Field Approach for Multicomponent Alloys with Extrapolation Scheme for Numerical Application," *Physical Review E,* Vol. 73, 2006, 066122-1 (9pp).
16. M. Militzer, "Phase Field Modeling of Microstructure Evolution in Steels," *Current Opinion in Solid State and Materials Scieince,* Vol. 15, 2011, pp. 106-115.
17. Thermo-Calc Software, FE2000 database, Stockholm, Sweden.

18. F. Fazeli and M. Militzer, "Application of Solute Drag Theory to Model Ferrite Formation in Multiphase Steels," *Metallurgical and Materials Transactions A,* Vol. 36A, 2005, pp. 1395-1405.